EKF based on two FDE schemes for GNSS Vehicle Navigation

Christophe Combettes, Christophe Villien

EKF based on two FDE schemes for GNSS Vehicle Navigation

Christophe Combettes
French Alternative Energies and Atomic Energy Commission
(CEA-LETI)
Grenoble, France
christophe.combettes@cea.fr

Christophe Villien
French Alternative Energies and Atomic Energy Commission
(CEA-LETI)
Grenoble, France
christophe.villien@cea.fr

***Abstract*— Due to the presence of outliers in GNSS measurements, a fault detection and exclusion module (FDE) is mandatory for applications such as vehicle navigation. In this paper, we propose a navigation processor with two different FDE. A first FDE based on the EKF innovation used when the convergence is ensured taking the benefit of the covariance matrix information. A second FDE with a standalone approach is used if the convergence is not ensured. Then, the performance of the proposed approach is evaluated with a large database of experiments.**

Keywords—GNSS positioning, RAIM, FDE

I. INTRODUCTION

A. Motivation and incitment

Although GNSS positioning is quite an old system, it recently gained some attention due to emerging applications like UAV and autonomous vehicles, or thanks to new technologies such as Galileo constellation, or consumer grade RTK and/or dual-band receivers which bring levels of accuracy and performances previously limited to expensive receivers, to everyone. The new paradigms offered by those evolutions, e.g. using low-cost receiver for accurate positioning, also requires to revisit some standard algorithms used for positioning in this context. In particular, satellite vehicle (SV) selection used to compute the position, velocity and time (PVT) solution is among the key aspects of the processing, because contrary to high-end receivers, the architecture of low-cost receiver neither benefits from Receiver Autonomous Integrity Monitoring (RAIM) modules, nor from selective antenna that significantly helps at mitigating reflected signals and outliers. As a consequence, SV selection performed at the navigation processor stage should receive some attention to ensure an accurate positioning, by using an efficient Fault Detection and Exclusion (FDE) algorithm.

B. Literature review

Several approaches have been proposed and compared in the literature [2], [3], [4], [5], and [6]. Most of them are based on Least Square (LS), Weighted Least Square (WLS) algorithms or robust estimators to compute the user or receiver position and its covariance matrix from pseudorange, pseudorange-rate or carrier phase measurements. Then, some statistical tests can be applied to the residuals of the computed solution to decide whether this latter is valid or based on some corrupted measurements. Those methods can be loosely classified into five approaches: the classic approach, the subset approach, the Multiple Hypothesis Solution Separation (MHSS) method, the robust methods and the EKF based method.

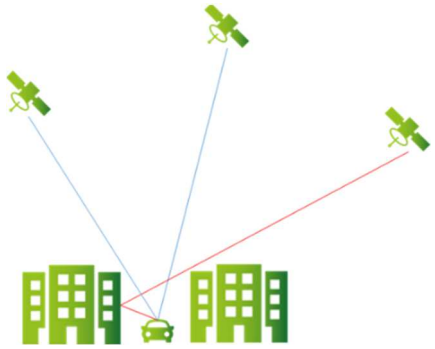

Fig. 1. LOS and NLOS paths of GNSS signals in urban environnement

The classic FDE [4], [5], [6], [8], is based on a double statistical test on the measurements residuals, called the global test and the local test. Assuming that all residuals are following a centred normal distribution, it comes that the weighted squared sum of the residuals follows a chi-2 distribution. The global test consists in comparing the latter statistic to the chi-2 distribution with a given probability of false alarm. If the empirical statistics of the residual are not matching with their corresponding covariance matrix, a failure is detected and an exclusion may be attempted based on a local test. Each measurement residual measurements is tested against its respective variance. For a given probability of missed detection, the largest unreliable residual is finally excluded. The global and local tests loop is repeated until the global test does not detect a failure. This approach is efficient to detect if there are outliers and a high redundancy, but the exclusion loop is not optimal due to LS sensibility to outliers. To prevent some wrong exclusions, a backward loop can be added. It consists in the reintroduction of the excluded measurement one-by-one until the new global test.

The second FDE approach is the “brute force” Subset testing based on measurements residuals [5], [7]. In the Subset testing approach, it is assumed that there are at most p outliers among a set of n measurements, and all the possible outlier-free subsets of n-p measurements are tested using a global criterion. The subset that passes the global test with the best scores is then selected. However, this approach is computationally intensive, and is not always tractable in real time. For instance, if there are 20 satellites in view and assuming 3 outliers would result into 1351 subsets to test. In order to reduce the computational time, other approaches have been developed such as range consensus (RANCO) [9], [10], and [11]. This approach is inspired by the random sample consensus (RANSAC), developed to overcome outlier issues in robust regression. The process starts from the selection of a subset of measurements, and then all remaining measurements are compared to this first solution. Then, residuals are compared to a threshold, and all the remaining

measurements are said to be inliers if they are below this threshold and outliers otherwise. The subset that gets the largest consensus is selected with all its inliers, its own outliers are rejected from the solution. The first selected subset is selected according to its Geometric Dilution of Precision (GDOP).

The third FDE approach, based on Subset testing processes is the MHSS which is part of the Advanced RAIM (ARAIM) [12], [13], [14]. The idea of this approach is to use the estimated position and its covariance matrix instead of the residuals measurement in the statistical test. Firstly, the position is estimated from a set of satellites. Then, for each possible subset, the position is estimated and compared to the estimated position from the whole set. The resulted residual positions are normalized with the estimated covariance matrix, and then a local test is achieved in order to detect a failure. An exclusion is attempted if a failure is detected with a subset approach. Like the previous subset approach, this one is also computationally intensive. To overcome the WLS sensitivity to outliers due to threshold effects, robust FDE approaches have been developed [4], [15]. A class of these robust methods is the iteratively reweighting approaches such as the Danish method [2], [5], [6], [7] or the Novel Integrity Optimized (NIORAIM) [16]. The main idea of the Danish method is to penalize the residuals with the largest values. If residuals are larger than a predefined threshold, their weight are reduced, e.g. the corresponding variance of the measurement covariance is increased. In order to minimize the missed detection or the false alarm, GNSS slopes is a parameter that can be checked, [15], [17].

In all approaches described above, the FDE process is standalone, that is to say essentially independent of the previous PVT solution. Some other FDE approaches based on the EKF previous solution [18] are using the prior information of the position to detect and eventually exclude outliers using innovation tests. Although those approaches are very efficient in terms of computational cost, they are less robust than standalone approaches because they assume previous PVT solution that is always reliable, and any erroneous measurement injected into the solution can cause the divergence of the algorithm due to its closed loop architecture.

C. Contribution and paper organization

The first fourth standalone approaches have sub-optimal performances due to the limited amount of prior information that can be used for SV selection and significant computational costs. To enhance the process, it is legitimate to use some prior information delivered by the predicted position but by closing the loop, but this increases the risk of algorithm instability. Indeed, if any outlier is not detected as such, it will be used to compute the PVT solution and possibly send it away from the true one, increasing the probability to select wrong measurement at the next epoch etc. That is why we propose in this paper a navigation processor based on an EKF algorithm that contains both a standalone FDE approach and a FDE based EKF approach. In the proposed approach, there is a switching between the two FDE based on the covariance matrix: considering that the navigation process is in a converged mode, the FDE based EKF innovation is used when the covariance matrix is below a threshold. If the covariance is above the threshold, the standalone FDE is used.

The paper is organized as follows: in a first part, the proposed navigation processor base on corrected pseudoranges is described with the two FDE methods. Finally, an experimental assessment based on a large database is provided and shows the efficiency of the proposed method.

II. Proposed navigation processor

A. State model

The positioning process is usually achieved by a WLS or an EKF and it consists of the estimation of the following state vector:

$$\boldsymbol{x}_a{}^T = \left(\boldsymbol{p}_a^{\gamma T} \quad \boldsymbol{v}_a^{\gamma T} \quad \delta\boldsymbol{\rho}_c^{aT} \quad \delta\dot{\rho}_c^a\right) \tag{1}$$

with $\boldsymbol{p}_a^{\gamma}$ and $\boldsymbol{v}_a^{\gamma}$ are the position and velocity of the receiver with respect to (w.r.t) a frame γ, $\delta\boldsymbol{\rho}_c^a$ is the vector containing receiver clock offsets of the different constellation, $\delta\dot{\rho}_c^a$ is the clock drift.

B. Measurement model

The raw pseudorange measurements from the satellite i and the receiver antenna a in l band are modelled as:

$$\tilde{\rho}_{a,R}^{i,l} = r_a^i + \delta\rho_{I,a}^{i,l} + \delta\rho_{T,a}^{i,l} - \delta\rho_c^{i,l} + \delta\rho_c^a + \delta\rho_{M,a}^{i,l} + \delta w_{\rho,a}^{i,l} \tag{2}$$

Where $\tilde{\rho}_{a,R}^{i,l}$ is the raw pseudorange measurement from the satellite i and the receiver antenna a, l is the carrier signal band; r_a^i is the geometric distance between the satellite and the antenna. The raw pseudo-range measurement is affected by errors such as the ionosphere delay $\delta\rho_{I,a}^{i,l}$, the troposphere delay $\delta\rho_{T,a}^{i,l}$, the satellite clock bias $\delta\rho_c^{i,l}$, the receiver clock bias $\delta\rho_c^a$ the multipath delay $\delta\rho_{M,a}^{i,l}$ and a random term $\delta w_{\rho,a}^{i,l}$ that represents the noise of the receiver. The geometric range is directly linked to the receiver antenna position:

$$r_a^i = \left\|\boldsymbol{p}_a^{\gamma} - \boldsymbol{p}_i^{\gamma}\right\|_2 + \delta\rho_i^{\gamma} \tag{3}$$

Where $\boldsymbol{p}_i^{\gamma}$ is the satellite position w.r.t γ, computed from ephemeris data and $\delta\rho_i^{\gamma}$ is the Sagnac effect. Navigation processor uses corrected pseudoranges computed from the raw pseudoranges, by removing ionosphere, troposphere and satellite clock delays using models [20] and ephemeris data. Corrected pseudorange $\tilde{\rho}_{a,C}^{i,l}$ can be modelled as:

$$\tilde{\rho}_{a,C}^{i,l} \approx r_a^i + \delta\rho_c^a + \delta v_c^a + \delta\rho_{M,a}^{i,l} \tag{4}$$

Where δv_c^a is a random variable that gathers all residual errors due to imperfect ephemerid based correction which are highly correlated over a short period of time (10s to 1mn) and the receiver noise which is essentially white. Although those residuals are time-correlated random process, they are generally represented as centered and white Gaussian noise [20] whose covariance depends on the satellite elevation $\theta_n^{a,i}$, the carrier to noise ratio $(C/N_0)_i$ and $\ddot{r}_a^s$ the range acceleration of between the antenna and the satellite:

$$\Sigma_{\boldsymbol{\rho}}(i,i) = \frac{1}{sin^2\left(\theta_n^{a,i}\right)}\left(\sigma_{\rho Z}^2 + \frac{\sigma_{\rho C}^2}{(C/N_0)_i} + \sigma_{\rho A}^2 \ddot{r}_a^{i\,2}\right) \tag{5}$$

$\sigma_{\rho Z}^2$ is the main component of the covariance, $\sigma_{\rho C}^2$ is the C/N_0 component and $\sigma_{\rho A}^2$ is the component related to the range acceleration. The Multipath term $\delta\rho_{M,a}^{i,l}$ is due to the reception of reflected signals which add a positive range error to the pseudorange measurements. In nominal conditions, this term is null, but in urban environments the occurrence of reflected signals is high and can lead to large positioning errors. Because multipath distribution cannot be handled efficiently by e.g EKF, objective of FDE is to detect their presence and discard the

measurement. Hence, measurement model of EKF assumes that no multipath is present:

$$\begin{aligned} \tilde{\rho}_{a,C}^{i,l} &= h_i(\boldsymbol{x}_a) + \delta v_{\rho,a}^{i,l} \\ h_i(\boldsymbol{x}_a) &= \left\| \boldsymbol{p}_a^{\gamma} - \boldsymbol{p}_i^{\gamma} \right\|_2 + \delta\rho_i^{\gamma} + \delta\rho_c^{a} \end{aligned} \tag{6}$$

The full model, containing all the corrected pseudoranges is:

$$\tilde{\boldsymbol{\rho}}_{a,C}^{l} = \boldsymbol{h}(\boldsymbol{x}_a) + \delta \boldsymbol{v}_{\rho,a}^{l} \tag{7}$$

$\tilde{\boldsymbol{\rho}}_{a,C}^{l}$ is the observation vector containing the current corrected pseudorange from all satellites in view, $\boldsymbol{h}$ is the mapping function containing defined by (5). The measurement noise $\delta \boldsymbol{v}_{\rho,a}^{l}$ is a random vector containing all noises $\delta v_{\rho,a}^{i,l}$. It is associated with the covariance matrix $\Sigma_{\boldsymbol{\rho}}$. In the estimation process, the model defined in (6) is linearized at the state estimate $\hat{\boldsymbol{x}}_a$:

$$\begin{aligned} \tilde{\boldsymbol{\rho}}_{a,C}^{l} - \boldsymbol{h}(\hat{\boldsymbol{x}}_a) &= H_a^{s,\gamma} \delta \boldsymbol{x}_a + \delta \boldsymbol{w}_{\rho,a}^{l} \\ H_a^{s,\gamma} &= \left. \frac{\partial \boldsymbol{h}}{\partial \boldsymbol{x}_a} \right|_{\boldsymbol{x}_a = \hat{\boldsymbol{x}}_a} \end{aligned} \tag{8}$$

Where Jacobian matrix $H_a^{s,\gamma}$ is the derivative of the mapping function $\boldsymbol{h}$, and $\delta \boldsymbol{x}_a$ is the state error. The same approach is adopted for the pseudorange rate measurements or the carrier phase measurements

C. Propagation step of the EKF

In the proposed EKF, the state vector $\boldsymbol{x}_a$ is composed respectively by the position, the velocity, the clock bias, the inter-constellation (i.e. GPS / GLONASS) clock bias and the clock drift (4). It is assumed here that there are only two constellations. The following propagation state model is used:

$$\begin{aligned} \delta \dot{\boldsymbol{x}}_a &= F \delta \boldsymbol{x}_a + \delta \boldsymbol{w}_{\boldsymbol{x}_a} \\ F &= \begin{bmatrix} 0_{3\times3} & I_{3\times3} & 0_{3\times3} \\ 0_{3\times3} & 0_{3\times3} & 0_{3\times3} \\ 0_{1\times3} & 0_{1\times5} & 1 \\ 0_{2\times3} & 0_{2\times3} & 0_{2\times3} \end{bmatrix} \end{aligned} \tag{9}$$

with $\delta \boldsymbol{w}_{\boldsymbol{x}_a}$ is noise processes of covariance noted $\Sigma_{\boldsymbol{w},\boldsymbol{x}_a}$. $0_{i\times j}$ and $I_{i\times i}$ are the i by j size null matrix and i by i identity matrix respectively. The a priori covariance matrix of the state vector is then propagated as:

$$\begin{aligned} P_{\delta x_a,n|n-1} &= F_d P_{\delta x_a,n-1} {F_d}^T + \Delta t \Sigma_{\boldsymbol{w},\boldsymbol{x}_a} \\ F_d &= I_{9\times9} + \Delta t F \end{aligned} \tag{10}$$

where Δt is the sampling period, and n correspond to n^{th} time iteration. The a-priori estimated state vector state $\hat{\boldsymbol{x}}_{a,n|n-1}$ is computed from the last a-posteriori estimated state vector $\hat{\boldsymbol{x}}_{a,n-1}$:

$$\hat{\boldsymbol{x}}_{a,n|n-1} = F_d \hat{\boldsymbol{x}}_{a,n-1} \tag{11}$$

D. Update step of the EKF

At time or iteration n, a corrected pseudoranges measurement is available. The innovation $\delta \boldsymbol{z}_n$ is computed as:

$$\delta \boldsymbol{z}_n = \tilde{\boldsymbol{\rho}}_{a,C,n}^{l} - \hat{\boldsymbol{\rho}}_{a,C,n|n-1}^{l} \tag{12}$$

Where $\tilde{\boldsymbol{\rho}}_{a,C,n}^{l}$ is the vector that contains the measurement at time n and $\hat{\boldsymbol{\rho}}_{a,C,n}^{l}$ is the vector that contains the estimated corrected pseudoranges from the a-priori state vector:

$$\hat{\boldsymbol{\rho}}_{a,C,n|n-1}^{l} = \boldsymbol{h}\left(\hat{\boldsymbol{x}}_{a,n|n-1}\right) \tag{13}$$

The update is realized thanks to the Kalman gain:

$$K = P_{\delta \boldsymbol{x}_a,n|n-1} H_a^{s,\gamma T} \left(H_a^{s,\gamma} P_{\delta \boldsymbol{x}_a,n|n-1} H_a^{s,\gamma T} + \Sigma_{\boldsymbol{\rho}} \right)^{-1} \tag{14}$$

Then the a-posteriori state is given by following update equations:

$$\begin{aligned} \hat{\boldsymbol{x}}_{a,n} &= \hat{\boldsymbol{x}}_{a,n|n-1} + K\left(\tilde{\boldsymbol{\rho}}_{a,C,n}^{l} - \hat{\boldsymbol{\rho}}_{a,C,n|n-1}^{l}\right) \\ P_{\delta \boldsymbol{x}_a,n} &= \left(I_{9\times9} - K H_a^{s,\gamma}\right) P_{\delta \boldsymbol{x}_a,n|n-1} \end{aligned} \tag{15}$$

Based on those two models, the covariance matrix of the estimated position will finally depend on the GDOP, the code pseudorange noise, the accuracy of the estimated delays (ionosphere, troposphere and satellite) and the satellite position estimation. However, outliers that are mainly caused by multipath propagation are not taken into account by those models, and must be excluded from the solution.

E. Fault detetction and exclusion

As previously said, the proposed FDE scheme is based on two independent FDE, depending on the algorithm convergence state which is reflected by the value of the covariance matrix and the value of the residuals. For normal operation, that is to say when the algorithm has a good convergence level indicated both by the amplitude of the residuals and the covariance matrix of the PVT solution, an innovation test will be used to detect and remove any outlier. In this mode, no additional PVT computation is required beyond the one delivered by the EKF prediction, minimizing the computational cost of the satellite selection process. When the algorithm has poor convergence, then a classical FDE test is used. The two FDE are using a global test first to validate the solution, eventually followed by local tests to exclude outliers if the global test failed.

1) FDE based on EKF innovation

This FDE is based on a classical innovation test applied to the innovation residuals of the EKF. During the update stage of the EKF the innovation is performed as computed as (3) by using the a-prior estimated state . $\hat{\boldsymbol{x}}_{a,n|n-1}$:

$$\boldsymbol{r}_{a,C,n}^{l} = \delta \boldsymbol{z}_n = \tilde{\boldsymbol{\rho}}_{a,C,n}^{l} - \hat{\boldsymbol{\rho}}_{a,C,n|n-1}^{l} \tag{16}$$

Those residuals are compared with their predicted covariance given by:

$$\Sigma_{\boldsymbol{r}} = H_a^{s,\gamma} P_{\delta \boldsymbol{x}_a,n|n-1} H_a^{s,\gamma T} + \Sigma_{\boldsymbol{\rho},\boldsymbol{FDE}} \tag{17}$$

Where $\Sigma_{\boldsymbol{\rho},\boldsymbol{FDE}}$ could be different to the noise measurement covariance matrix given (5). In (5), it is a covariance matrix used for accuracy whereas the covariance matrix used in (17) is designed for integrity [8]. In order to detect multipath, $\Sigma_{\boldsymbol{\rho},\boldsymbol{FDE}}$ should not contains the multipath uncertainties contrary to the model (7), especially in the term $\sigma_{\rho Z}^2$. Indeed, the aim of the FDE is to detect outliers which are in most of the cases reflected signals. Then, all residuals are compared to their predicted covariance

$$\left| \boldsymbol{r}_{a,C}^{l}(i) \right| < k_{normal} \sigma_r(i) \tag{18}$$

with $\sigma_r(i) = \sqrt{\Sigma_r(i,i)}$ and k_{normal} a constant to fix. If the residual i pass the test, then the measurement i will be included in the solution, otherwise it will be discarded.

2) FDE based on standalone WLS

TABLE I. NAVIGATION PROCESS WITH DOUBLE FDE

- Initialization: *Set state and covariance* $\boldsymbol{x}_{a,0}$, $\boldsymbol{P}_{a,0}$ *and Convergence Flag=0*
- State propagation at time n: *Compute* $\hat{\boldsymbol{x}}_{a,n|n-1}$ *and* $P_{\delta \boldsymbol{x}_a,n|n-1}$ *from (10) and (9) respectively*
- Estimate corrected pseudoranges: *Compute* $\hat{\boldsymbol{\rho}}^{l}_{a,C,n|n-1}$ *from (13), Compute* $\Sigma_{\boldsymbol{\rho}}$ *from (5)*
- Fault detection and exclusion if Convergence Flag=1: *Compute* $\delta \boldsymbol{z}_n$, $\Sigma_{\boldsymbol{r}}$ *from (16) and (17); Select satellites with the test (18)*
- Fault detection and exclusion if Convergence Flag=0: *Compute position* $\hat{\boldsymbol{x}}^{wls,k}_{a,n}$ *from the process (19), (20) and (21); Compute residuals and covariance* $\boldsymbol{r}^{l,wls}_{a,C,n}$, $\Sigma_{\boldsymbol{r}}$ *from (22) and (23); Select satellites with the global test (25), and the local test with (26)*
- State update: *Compute residual* $\delta \mathbf{z}_n$ *from (12) with the selected satellites; Compute* $\hat{\boldsymbol{x}}_{a,n}$ *and* $P_{\delta \boldsymbol{x}_a,n}$ *from (14) and (15)*
- Convergence flag update: *Update Convergence Flag from (27)*

If the navigation processor has a poor convergence state, then a classical FDE approach will be used. The residuals test method is based on the analysis of the WLS algorithm which is implemented in the FDE. The WLS is initialized with the estimation from the navigation solver:

$$\hat{\boldsymbol{x}}^{wls,0}_{a,n} = \hat{\boldsymbol{x}}_{a,n} \tag{19}$$

The iterative process of the WLS is defined by the following equations:

$$\begin{aligned} P^{wls,k}_{\delta \boldsymbol{x}_a,n} &= \left({H_a^{s,\gamma}}^T {\Sigma_{\boldsymbol{\rho}}}^{-1} H_a^{s,\gamma} \right)^{-1} \\ \delta \boldsymbol{x}^{wls,k}_{a,n} &= P^{wls,k}_{\delta \boldsymbol{x}_a,n} {H_a^{s,\gamma}}^T {\Sigma_{\boldsymbol{\rho},\boldsymbol{FDE}}}^{-1} \left(\tilde{\boldsymbol{\rho}}^{l}_{a,C} - \boldsymbol{h}\left(\hat{\boldsymbol{x}}^{wls,k}_{a,n} \right) \right) \\ \hat{\boldsymbol{x}}^{wls,k+1}_{a,n} &= \hat{\boldsymbol{x}}^{wls,k}_{a,n} + \delta \boldsymbol{x}^{wls,k}_{a,n} \end{aligned} \tag{20}$$

To condition are used to stop the WLS algorithm:

$$\left\| \delta \boldsymbol{x}^{wls,k}_{a,n} \right\|_2 < T_{wls} \text{ or } k > k_{max} \tag{21}$$

Where T_{wls} is a threshold on the state error and k_{max} is the maximum number of iteration used in the WS. Then, the residuals are defined by:

$$\boldsymbol{r}^{l,wls}_{a,C,n} = \tilde{\boldsymbol{\rho}}^{l}_{a,C,n} - \boldsymbol{h}\left(\hat{\boldsymbol{x}}^{wls,k_{max}}_{a,n} \right) \tag{22}$$

And their associated covariance by:

$$\Sigma_{\boldsymbol{r}} = \Sigma_{\boldsymbol{\rho},\boldsymbol{FDE}} - H_a^{s,\gamma} P_{\delta x_{a,wls}} {H_a^{s,\gamma}}^T \tag{23}$$

Assuming that the measurements are matching the models (3) they should be distributed as:

$$T^{wls}_n = {\boldsymbol{r}^{l,wls}_{a,C,n}}^T {\Sigma_{\boldsymbol{r}}}^{-1} \boldsymbol{r}^{l,wls}_{a,C,n} \sim \chi^2_{m-p} \tag{24}$$

Where χ^2_{m-p} is the chi-2 distribution with *m-p* degree of freedom (number of measurements minus number of states). From this statistic, it is possible to construct a global test to detect if there are outliers:

$$T^{wls}_n < k_{poor,GT} \chi^2_{m-p}(1-\alpha) \tag{25}$$

With α false alarm probability, and $k_{poor,GT}$ a constant to set. If the global test fails an exclusion must be attempted. As for the innovation test, residuals are compared to their associated covariance

$$\left| \boldsymbol{r}^{l}_{a,C}(i) \right| < k_{poor,LT} \sigma_r(i) \tag{26}$$

with $\sigma_r(i) = \sqrt{\Sigma_r(i,i)}$ and $k_{poor,LT}$ a constant set by the designer.

This standalone FDE is only used when the navigation processor is not in converged mode. This process ensure to select satellites without outlier with a reduced risk. However, the exclusion step is not as efficient as the FDE based on EKF innovation. The converged mode is based on the comparison of the covariance matrix to threshold:

$$max\left(P_{\delta \boldsymbol{x}_a,n} \right) < T_{P_{\delta x_a}} \tag{27}$$

Where $P_{\delta \boldsymbol{x}_a,n}$ is the covariance matrix from the navigation solver and $T_{P_{\delta x_a}}$ is a fixed threshold. The proposed navigation process algorithm is presented in the following pseudocode, Table 1.

III. EXPERIMENTAL ASSESSMENT AND RESULTS

A. Description of the experimental assessment

In this experimental assessment part, several algorithms are evaluated. The proposed navigation processor based on double FDE, the classical FDE scheme, the Subset testing, and a robust approach named Danish method. The measurements are issued from the receiver NEO-M8P from Ublox. The reference system is an Inertial navigation system integrated with a dual antenna GNSS RTK from SBG (equinox 2D). The reference trajectory is generated from Qinertia post-processing software providing a centimetre accuracy. All these equipment are embedded on the roof of the vehicle, Fig.2. The full database is composed of 80 sessions, each of them having a duration ranging from 10 minutes and up to 1 hour. Database addresses various scenarios like urban environments, highways, country road.

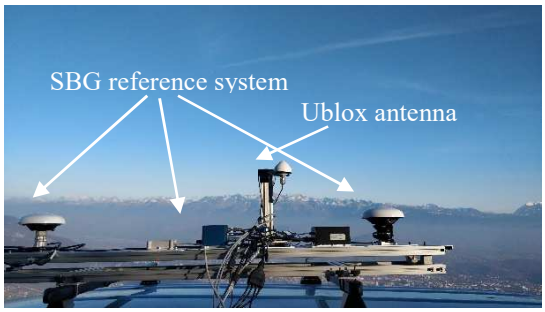

Fig. 2. Illustration of the testbench used for fieldtests with the reference system (SBG) and the system under test (ublox) mounted on the roof of the vehicle

B. Results

To highlight the benefits of using a FDE in a navigation process based on GNSS, the results of a navigation process without a FDE are also added. The metrics used to compare navigation processes are the root mean square error and the P99, i.e. the 99th centile, which gives information about the tail of the distribution error. The processing time of a data file with a duration time of 1104s is added in order to compare the computation time performances of the different methods. The parameters of the computer used to perform the following results are: processor Intel(R) Core(TM) i5-8250U CPU: 1.80 GHz, and RAM: 64 bits, 32 GB. Navigation process algorithms are compiled in C from a Matlab implementation. The results are given in the Table II. The different FDE improve the navigation processor by a factor from 1.5 to 2 and reduce the divergence

risk of the navigation process. The combination of a double FDE improves the accuracy of the navigation process while reducing the computation cost: 2.8m (rms) versus 3.38m (rms) for the Subset testing method. Indeed; the FDE based on EKF innovation is only a test from the EKF innovation and its covariance, which are already computed. The others FDE need a higher computation time than the FDE based EKF, because the process is independent to the navigation solution and need to solve the position of the receiver. Of course some methods are less computationally expensive than the others, e.g. Danish method vs Subset testing. Nevertheless, the FDE based on EKF is interesting on this point. In terms of accuracy, the FDE based on EKF innovation improves the accuracy of the navigation process. The FDE based on EKF innovation uses another source of information with the covariance matrix of the innovation. This latter provides us the accuracy of the computed innovation. Then, the test is simply the consistency checking of the innovation to its covariance matrix. Therefore, the accuracy is improved by a better satellite selection/rejection. The improvements are clearly apparent on the P99 which gives us an information about the tail of the error distribution. The proposed approach rejects large residuals which may be not rejected by other approaches. However, the FDE based on EKF innovation must go with a standalone FDE approach, especially in case of poor convergence. Indeed, in this case, the position error could not be reflected by the covariance matrix, which lead to missed detections or false alarms. In the next paragraph, a case of multipath is analysed in order to show the benefit of the use of double FDE. The proposed method is compared to the Subset testing method, because this latter is relatively efficient to isolate faulty measurements.

TABLE II. RESULTS OF THE NAVIGATION PROCESSES

Algorithms	*Error rms (m)*	*P 99(m)*	*Process. Time(s)*
w/o FDE	5.02	Inf	2.84
Classic FDE	3.62	9.69	7.66
Classic FDE+ EKF based FDE (Proposed Method)	2.80	6.93	4.31
Subset Testing FDE	3.38	8.65	13.98
Danish method FDE	3.15	8.24	7.00

C. *Analysis: case of multipath*

In case of multipath, a positive delay is added to the GNSS raw measurements compared to the nominal conditions. If this delay is not treated in the EKF, it will lead the navigation process to a failure. In case of only one faulty measurements and if the geometry is not too bad e.g. GDOP<20 [21], all FDE are able to detect a fault and exclude the faulty satellite. The challenge comes when serval faulty measurements occur at the same epoch. In this configuration, the detection of a failure is still achievable for all FDE but the exclusion become tricky. Indeed, all residuals become comparable in size and then it is not possible to distinguish the faulty measurements to the no-faulty ones. To underline the effect of multiple multipath, a configuration is selected where serval satellites measurements are affected by multipath or important faults. For example at t = 2305.4s from a file of our database where GPS 62, 6, 14 and 31 and GLO (Glonass) 5 and 15 are faulty measurements. The residuals of the pseudoranges computed from the reference trajectory are presented in Fig.3. The residuals of the Subset testing are given in Fig.4. At t=2305.4, the Subset testing failed to exclude all faulty measurements: Faulty measurements GLO 5 and 15 are kept to the solution though they have high residuals. However, the selected satellites from the Subset testing succeed in the global test (24). The missed detection seems to originate from two elements: Firstly, the residuals of GLO 5 and GLO 15 are closed in size, 112m and 119m respectively. Secondly, the geometry is poor, especially on the inter-constellation clock bias. Indeed the value of GDOP is 19.9, which is not fair but also not poor [21]. The line of sight vectors of the two satellites are closed: ${u_{GLO\_5}}^T = (0.20 \quad 0.75 \quad -0.63)$ and ${u_{GLO\_15}}^T = (0.22 \quad 0.81 \quad -0.55)$. It means that there is not redundancy for the estimation of the inter-constellation bias. Thus, the multipath bias is totally absorbed by the estimated inter-constellation clock bias in the WLS process used in the Subset testing: the inter-constellation clock bias varies from 11m at t=2305.2 (previous epoch) to 104m at t=2305.4. Because the global test is not rejected, these two satellites are finally selected as correct measurements Fig.4, and the navigation process solution (EKF) based on Subset testing gradually drifts from the reference trajectory, Fig.5.

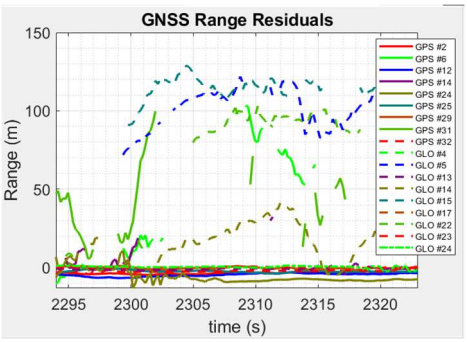

Fig. 3. GNSS (all) range residuals computed from the reference trajectory

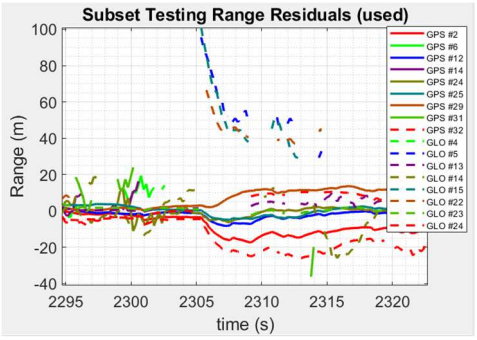

Fig. 4. GNSS (used only) range residuals computed from a navigation process with Subset testing FDE

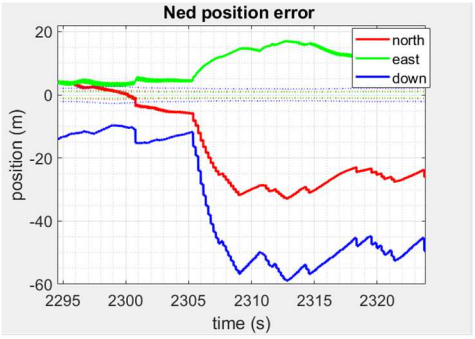

Fig. 5. Position error w.r.t. Ned frame of a navigation process with Subset testing FDE

The proposed navigation process based on Classic and EKF FDE takes the advantage of the covariance matrix information. This latter contains the knowledge of the accuracy of the estimated solution. Thus, the covariance matrix of the

innovation can be estimated and used to check the consistency of innovation values. At t=2305.4s, innovation of the GLO 5 and GLO 15 is 107.27m and 113.31m, respectively. The corresponding standard deviation are in contrast evaluated at 5.43m and 5.48m. Therefore, the values of innovation are not consistent with respect to the covariance matrix. The measurements of the satellite GLO 5 and GLO 15 are rejected from the navigation solution, Fig.6. Then the positioning solution is not impacted by these two outliers, Fig.7.

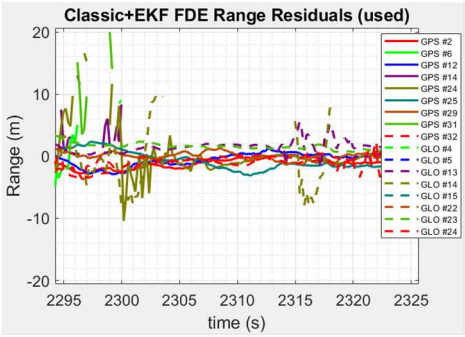

Fig. 6. GNSS (used only) range residuals computed from a navigation process with Classic + EKF FDE

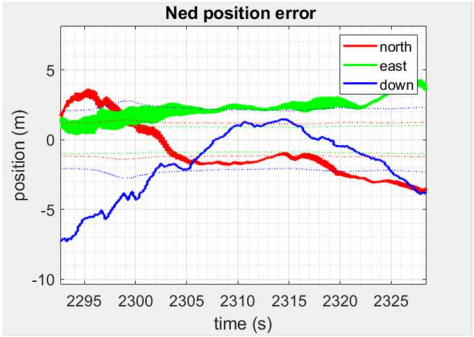

Fig. 7. Position error w.r.t. Ned frame of a navigation process with Classic FDE and EKF FDE

IV. Conclusions

In this paper, a navigation process with a FDE scheme that switch from a classic FDE to a FDE based on EKF innovation when the convergence of the navigation process is established, i.e. the covariance matrix is below a threshold is implemented This approach uses the a priori information contained in the covariance matrix in order to check the consistency of the residuals. The proposed method is then compared with a large database to different FDE schemes from the state of art. The performances of the proposed method are 2.8m (rms) and a P99 of 6.93m versus a 3.18m (rms) and a P99 of 8.24m for the Danish method. However, in case of poor convergence, the proposed approach will use the classic FDE scheme, which is not optimal in case of multiple faulty measurements. In this case different elements such that such as the GDOP and/or the seperability [5] could be interesting to improve the failure detection and exclusion.

References

[1] W. Y. Ochieng, K. Sauer, D. Walsh, G. Brodin, S. Griffin, and M. Denney, "GPS integrity and potential impact on aviation safety," Journal of Navigation, vol. 56, no. 1, pp. 51–65, 2003.-

[2] P. Zabalegui, G. De Miguel, A. Pérez, J. Mendizabal, J. Goya and I. Adin, "A Review of the Evolution of the Integrity Methods Applied in GNSS" IEEE Access vol. 8, pp. 45813-45824, 2020

[3] N. Zhu, J. Marais, D. Bétaille and M. Berbineau, "GNSS Position Integrity in Urban Environments: A Review of Literature" in IEEE Transactions on Intelligent Transportation Systems, vol. 19, no. 9, pp. 2762-2778, 2018,

[4] N. Knight, J. Wang, "A Comparison of Outlier Detection Procedures and Robust Estimation Methods in GPS Positioning". Journal of Navigation, vol 62. pp. 699-709, 2009

[5] A. Angrisano, C. Gioia, S. Gaglione,G. Core "GNSS Reliability Testing in Signal-Degraded Scenario", International Journal of Navigation and Observation, vol 2013, article ID 870365, 2013

[6] H. Kuusniemi, A. Wieser, G. Lachapelle and J. Takala, "User-level reliability monitoring in urban personal satellite-navigation" in IEEE Transactions on Aerospace and Electronic Systems, vol. 43, no. 4, pp. 1305-1318, 2007

[7] H. Kuusniemi, G. Lachapelle, "GNSS Signal Reliability Testing in Urban and Indoor Environments", Proceedings of the 2004 National Technical Meeting of The Institute of Navigation, San Diego, CA, pp. 210-224, 2004.

[8] D. Salos, "Integrity monitoring applied to the reception of GNSS signals in urban environments", Ph.D. thesis, University of Toulouse, Toulouse, FR, 2012

[9] J. Zhao, C. Xu, Y. Jian, et P. Zhang, "A Modified Range Consensus Algorithm Based on GA for Receiver Autonomous Integrity Monitoring", Mathematical Problems in Engineering, vol. 2020, p. 8969032, 2020.

[10] S.Radicella, G Castaldo, A. Angrisano, S. Gaglione, S. Troisi, "P-RANSAC: An Integrity Monitoring Approach for GNSS Signal Degraded Scenario", International Journal of Navigation and Observation, vol 2014, article ID 173818, 2014.

[11] G.Schroth, M. Rippl, A. Ene , J. Blanch, B. Belabbas , T. Walter , P. Enge, M. Meurer, "Enhancements of the Range Consensus Algorithm (RANCO)", DLR and Standford University, 2008 [Online]. Available: http://web.stanford.edu/group/scpnt/gpslab/pubs/papers/Schroth_IONGNSS_2008.pdf

[12] Y. Zhai, M. Joerger, and B. Pervan, "Fault exclusion in multi-constellation global navigation satellite systems," Journal of Navigation, vol. 71, no. 6, pp. 1281–1298, 2018

[13] J. Blanch, T. Walter, P. Enge, Y. Lee, B. Pervan, M. Rippl, A.Spletter, "Advanced RAIM user Algorithm Description: Integrity Support Message Processing, Fault Detection, Exclusion, and Protection Level Calculation", Standford University, 2012 [Online]. Available: http://web.stanford.edu/group/scpnt/gpslab/pubs/papers/Blanch_et_al_IONGNSS_2012_B5_nr7_post_submission_rev3.pdf

[14] M. Joerger, F.C. Chan, B. Pervan, (2014) "Solution Separation Versus Residual-Based RAIM", Journal of the Instiute of Navigation, vol 61, no 4, pp 273– 291, 2014

[15] W. Wang, Y Xu. "A Modified Residual-Based RAIM Algorithm for Multiple Outliers Based on a Robust MM Estimation". Sensors 20, 5407, 2020,

[16] A.J. Joseph, G. Lachapelle, "Applying the Genetic NIORAIM Algorithm to High Sensitivity GNSS Receivers Operating Indoor", Proceedings of the 22nd International Technical Meeting of the Satellite Division of The Institute of Navigation, Savannah, GA, September 2009.

[17] J. Zhao, D. Song, C. Xu and X. Zheng, "A Modified LSR Algorithm Based on the Critical Value of Characteristic Slopes for RAIM," IEEE Access, vol. 7, pp. 70102-70116, 2019,

[18] N. Zhu, D. Betaille, J. Marais and M. Berbineau, "Extended Kalman Filter (EKF) Innovation-Based Integrity Monitoring Scheme with C / N0 Weighting", 2018 IEEE 4th International Forum on Research and Technology for Society and Industry (RTSI), 2018.

[19] Y. Sun. "RAIM-NET: A Deep Neural Network for Receiver Autonomous Integrity Monitoring" Remote Sensing, vol 12, no. 9: 1503, 2020

[20] P.D. Groves, *Principles of GNSS, Inertial, And Multisensor Integrated Navigation Systems,* Aretch House, Second Edition, 2013

[21] Ch. Raja Sekhar, V.B.S. Srilatha Indira Dutt, G. Sasibhushana Rao, "GDoP estimation using Simulated Annealing for GPS and IRNSS combined constellation", Engineering Science and Technology Journal, vol 19,issue 4, pp 1881-1886, 201